Science of the Total Environment 667 (2019) 500–510

Contents lists available at ScienceDirect

Science of the Total Environment

journal homepage: www.elsevier.com/locate/scitotenv

Making global river ecosystem health assessments objective, quantitative and comparable

C. Zhao [a,g], T. Pan [b], T. Dou [c], J. Liu [d], C. Liu [a,*], Y. Ge [c], Y. Zhang [b], X. Yu [b], S. Mitrovic [e], R. Lim [f]

[a] College of Water Sciences, Beijing Normal University, Beijing Key Laboratory of Urban Hydrological Cycle and Sponge City Technology, Beijing 100875, PR China
[b] School of Geography, Beijing Normal University, Beijing 100875, PR China
[c] Jinan Survey Bureau of Hydrology and Water Resources, Jinan 250013, PR China
[d] School of Environmental Science and Engineering, Southern University of Science and Technology, Shenzhen, 518055, PR China
[e] School of Life Sciences, Faculty of Science, University of Technology, Sydney, NSW 2007, Australia
[f] School of the Environment, Faculty of Science, University of Technology, Sydney, NSW 2007, Australia
[g] ICube, UdS, CNRS (UMR 7357), 300 Bld Sebastien Brant, CS 10413, 67412 Illkirch, France

HIGHLIGHTS

- We present a new method for quantitatively and objectively assessing river health.
- It allows results to be compared over time and in different river systems.
- UAVs and satellite images aid obtaining objective measurements of river conditions.
- This method can be taken for river ecosystem assessment globally.

GRAPHICAL ABSTRACT

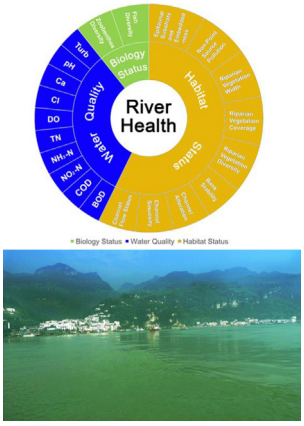

ARTICLE INFO

Article history:
Received 30 November 2018
Received in revised form 21 February 2019
Accepted 24 February 2019
Available online 27 February 2019

Editor: Jay Gan

Keywords:
River ecosystem health
Habitat quality
Biota
Hydrology
Water quality

ABSTRACT

Assessing and comparing global river ecosystem health in an objective and quantitative way remains a major challenge. In this study the widely-used semi-quantitative methods Rapid Biological assessment Protocols (RBPs) was used to determine the health of rivers. The findings were then compared to the results derived from our new UAV (Unmanned aerial vehicles) orthophotographic imagery method. This method quantitatively and objectively assesses river ecosystem health. As a comparison, our method was used to quantitatively measure distance and areas of a range of hydrological and biological attributes thus improving the accuracy of distance- and area-related indices, consequently avoiding subjective errors in these estimations that is fraught in methods like the RBPs. To strengthen the objectivity of the assessment the weights of these indices were objectively determined using the entropy weighting method. This new method was then tested using 9551 UAV orthophotographs taken over six field campaigns. It performed satisfactorily, showing that in our study area the health status of mountain rivers was the best with the highest score of 0.94 out of 1.0. Temporally, the health of the river was better in summer (0.65) compared with that in autumn (0.40). Changes in river ecosystem health

* Corresponding author.
E-mail addresses: pacorrespondence@126.com, liucm@igsnrr.ac.cn (C. Liu).

https://doi.org/10.1016/j.scitotenv.2019.02.379

were driven by variations in biology and water quality. In contrast the outputs of RBPs, especially in relation to distance and area indices, had ~ 20% uncertainty due to visual errors and subjectivity in estimations by observers. The UAV orthophotographic imaging method proposed in this study can improve the ability to compare the health of rivers across different periods and regions throughout the globe.

1. Introduction

Healthy rivers are crucial to the survival of humanity (Wei et al., 2009; Palmer and Febria, 2012; Zhu et al., 2014), as they not only provide water for domestic, industrial and agricultural uses but are also essential for ecological services to commerce, transportation, recreation and other activities (Deng et al., 2015). As rivers are an important component of the terrestrial environment, they are vulnerable to human impacts, leading to changes in water quality and biological diversity (Fendorf et al., 2010; Grafton et al., 2013).

Globally, climate change and disruptive human activities have altered water cycles and river environments (Palmer, 2010; Luo et al., 2013; Poff et al., 2016), such as hydrological conditions, pollutant loads, and habitat attributes, which pose a serious threat to ecosystem health and services (Marzin et al., 2014; Zhu et al., 2014; Zhao et al., 2018). The degradation of the health of rivers has become a major crisis for human survival and sustainable development (Tang et al., 2002; Acreman and Dunbar, 2004; Zhu et al., 2014). Thus research to seek approaches to maintain and protect the health of riverine ecosystems is needed.

River health is often defined as the health of its ecosystem by some researchers (Cairns Jr and McCormick, 1992; Cairns et al., 1993; Schofield and Davies, 1996; Costanza et al., 1997; Pan et al., 2015); while others define it more anthropocentrically to include ecosystem services to humans particularly in the context of development of the local economy and society (Rapport, 1989; Meyer, 1997; Peng et al., 2015). The goal of our paper is to assess the health of river ecosystems, which is the first step towards its protection. Such studies are of global concern for researchers, governments and other stakeholders (Clarke et al., 1996; Clarke and Hering, 2006; Hughes et al., 2000; Marzin et al., 2014). Consequently, many theories have been put into practice over the last few decades. Assessment of a river ecosystem needs to integrate physical, chemical and biological variables to characterize the threats to its health in a sufficiently robust way (Boulton, 1999; O'Brien et al., 2016). Among these variables, the quality of habitat, e.g., riparian vegetation, instream hydrological regime, and water quality determines the structure of river ecosystem communities. Therefore, accurately assessing the health of the habitat is core to gaining insights to the condition in the river. A number of methods have been developed. Hankin and Reeves (1988) developed a visual method for estimating habitat area in forested salmonid streams. The USEPA produced a rapid physical habitat assessment for use throughout the U.S., which evolved into the Rapid Bioassessment Protocols (RBPs) (Plafkin et al., 1989). In the same year Rankin (1989) published a qualitative habitat evaluation index (QHEI). Both these protocols were refined in subsequent years (Barbour et al., 1999; Rankin, 2006). Among these methods, the RBPs was one of the most widely used methods due to its efficiency and effectiveness (Barbour et al., 1999; Hughes et al., 2010; Blue, 2018). RBPs can reflect overall ecological integrity and directly assess the status of a waterbody (Stephens and Farris, 2004). From the perspective of habitat and biology, RBPs select 13 indicators including flow velocity, water depth, river bed stability and river channel morphology to construct a river health assessment system (Barbour et al., 1999). However, previous methods used for habitat health assessment have been semi-quantitative, and there exist few reports on habitat health assessment (Stubauer et al., 2010; Mouton et al., 2012; Marteau et al., 2017), thus generating great uncertainty for assessing the health of rivers.

Traditionally, indices of river ecosystem health assessment have been evaluated by a scoring method and divided into four levels: 'optimal', 'suboptimal', 'marginal', and 'poor', with possible scores of 1 through 4 based on fuzzy descriptive evaluation criteria at each level (Barbour et al., 1999; Deng et al., 2015). This method can generally describe the condition of a river but cannot quantitatively measure river ecosystem health. In addition, using only qualitative and descriptive indices can result in serious bias in assessment results because the assessment relies on the expertise of assessors, which varies from person to person. Thus comparing the health of rivers across regions would be constrained.

To reduce the bias in estimating river ecosystem health – especially habitat health, a more quantitative measurement of attributes especially distance and area is urgently needed. Unmanned aerial vehicles (UAVs) are a new measurement platform developed in recent years. UAVs can measure distances and areas very accurately, making them a promising tool for ecological restoration and river monitoring studies at reach scales (Dunford et al., 2009; Carbonneau et al., 2012; Dufour et al., 2013; Messinger et al., 2016). Physical habitat, as an important component of river ecosystem health, can therefore be accurately monitored using UAVs (Marteau et al., 2017).

The purpose of this paper is to present a new method to assess the health of rivers using quantitative data sources and newly developed index-calculating methodologies. By using this quantitative and objective method, the subjectivity encountered in previous methods was greatly reduced and poor comparability of these assessments temporally and spatially was also overcome.

2. Study area

Jinan (36.0–37.5° N, 116.2–117.7° E) city, located in eastern China, is bordered by Mount Tai to the south and traversed by the Yellow River. It has steeper topography in the south than in the north (Fig. 1). The city spans hilly areas, piedmont clinoplain and alluvial plains from south to north. The elevation within the area ranges from −66 to 957 m above sea level, with highly contrasting relief (Cui et al., 2009; Zhang et al., 2010; Zhao et al., 2015a). The semi-humid continental monsoon climate in the city area is characterized by cold, dry winters and hot, wet summers. The average annual precipitation is 636 mm, 75% of which falls during high-flow periods. The average annual temperature was 14.3 °C over the survey period (2014–15); the average monthly temperature was highest in July, ranging from 26.8 to 27.4 °C; and the lowest was in January, ranging from −3.2 to −1.4 °C (Zhao et al., 2015a; Zhao et al., 2015b). Jinan is the first pilot city reconstructed as a healthy water ecology precinct in China. With rapid industrial development and urbanization in recent decades, water resources in Jinan city have become severely polluted and reduced in quantity through extraction (Zhang et al., 2007a, 2007b). As a result, water safety and human health are increasingly threatened (Hong et al., 2010). To mitigate water safety and human health concerns, assessment and restoration of its river ecosystem is urgently needed.

To explore an effective method to assess and restore the health of this river system, 59 routine monitoring sites were set up across the drainage network (Fig. 1). In this study, four representative sites (key site in Fig. 1) among 59 routine monitoring sites were selected to represent different river characteristics: J1 was located in a mountainous river with little human activity, while J5 represented a mountainous river with intensive human activity; J16 represented a river plain sub-

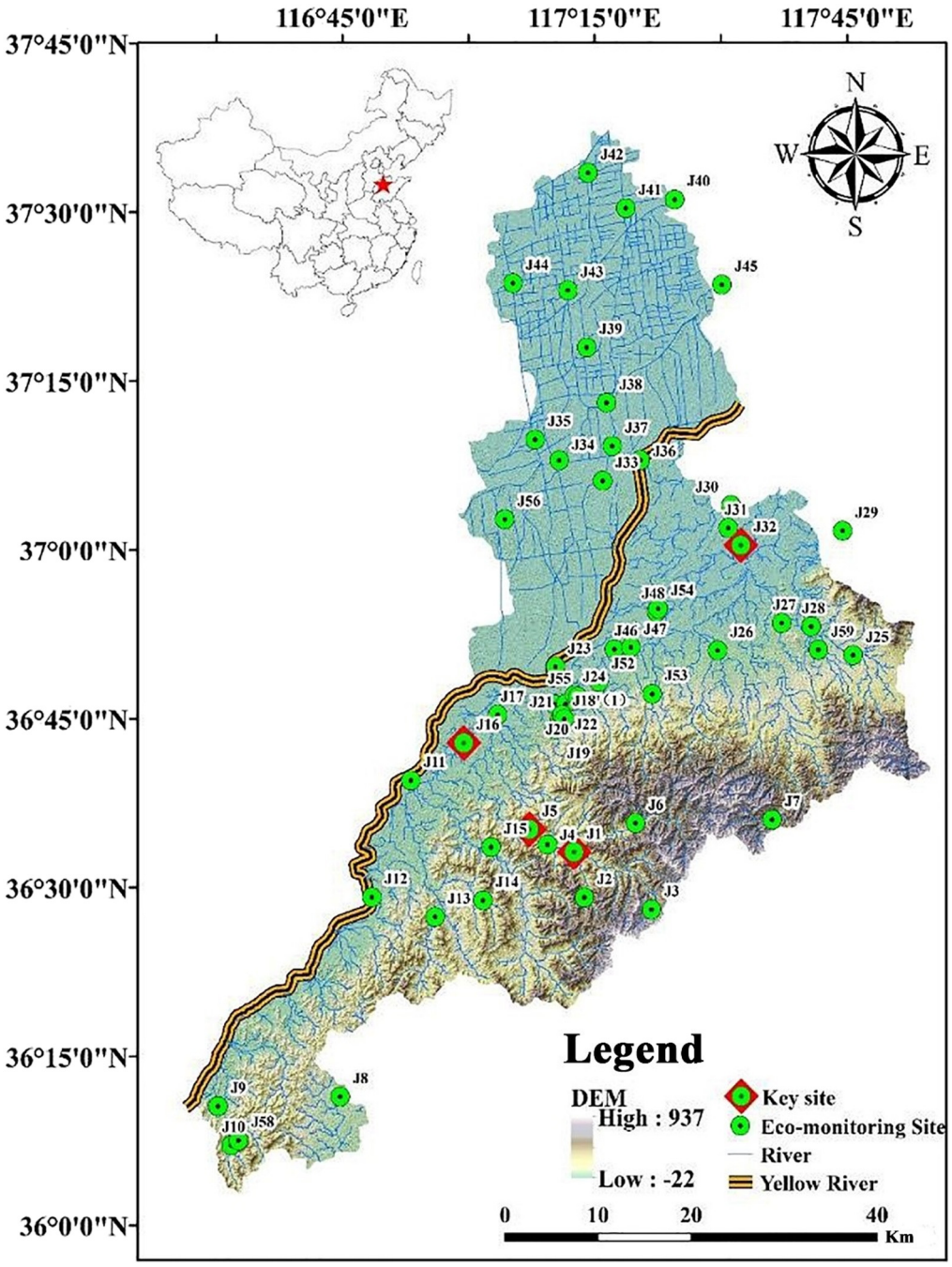

Fig. 1. Study area of Jinan City with locations of 59 routine limnological monitoring stations (eco-monitoring site); the four key sites can represent different river characteristics in the study area.

catchment occupied by farmland, while J32 was a river plain sub-catchment with sparse farmland (Fig. 1).

3. Methods and data

3.1. Methods

To comprehensively assess the health of the river, we set up an assessment system consisting of 3 first-level indices i.e., habitat, biological status, and water quality, where nine, three and ten second-level attributes, respectively were integrated (Fig. 2). Weights for each of the identified index at both levels were then determined using the entropy method. The entropy method was used to avoid subjectivity in calculating the weight of each index (Hao and Singh, 2013; Zhao et al., 2015a). Based on these calculations the weighted sum of second-level indices should equal the weight value of their respective first-level index. The weighted sum of the first-level indices was then used to determine the health of the river.

3.1.1. Conversion of physical habitat indices from semi-quantitative to quantitative values with newly presented formulae for assessing the health of the river

Ten traditional semi-quantitative indices derived for the RBPs were converted to nine quantitative ones (Indices 1–9 in Table 1) using UAV orthophotographs, which provided more accurate and objective assessment outputs. Hydrological parameters of velocity, depth and streamflow were used to assess the status of the physical habitat. In addition, a new index (Index 10 in Table 1) was developed to quantify the

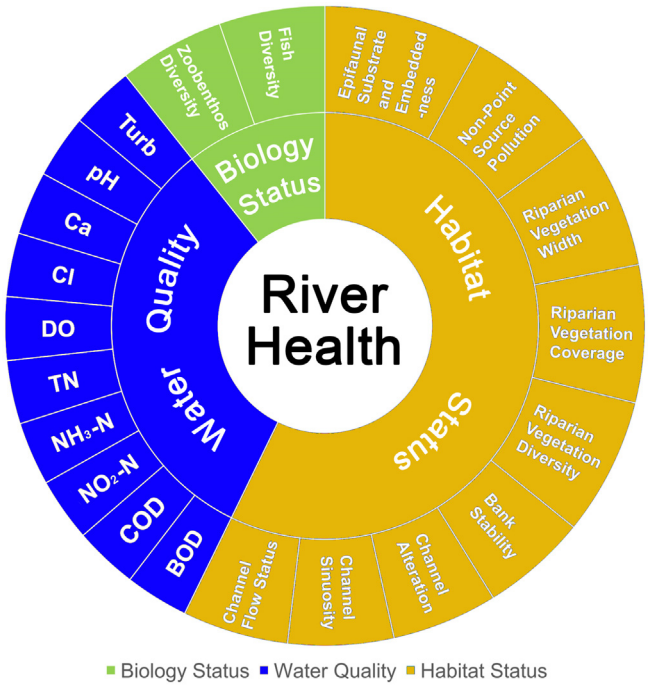

Fig. 2. River ecosystem health assessment system. The biology status (green), water quality (blue) and habitat status (orange) were the first-level indices. Based on their second-level indices in the outer-most layer, the three fist-level indices were integrated to assess the health of the river. (For interpretation of the references to color in this figure legend, the reader is referred to the web version of this article.)

impact of non-point source pollution on river ecosystem health. Distance and area were measured using ESRI ArcGIS[1] and Google Earth Pro.[2] Detailed formulae are listed in Table 1.

Epifaunal Substrate and Embeddedness (Index 1 in Table 1) includes the relative quantity and variety of natural structures in the stream, such as cobbles, large rocks, fallen trees, logs and branches, and undercut banks, available as refugia, or as sites for feeding-spawning-nursery functions of aquatic macro-fauna (Barbour et al., 1999). Epifaunal substrate and embeddedness were evaluated in this study using the Margalef index (Margalef, 1958; Gamito, 2010), wherein the number of individuals was replaced with the area that can be easily obtained from UAV orthophotographs over the dry season.

Velocity and Depth Regime (Index 2 in Table 1) includes patterns of velocity and depth as an important attribute of habitat diversity (Barbour et al., 1999). Their variance was used to assess the diversity of water depth and velocity. The average of normalized variance was the final score for velocity and depth regime.

Channel Flow Status (Index 3 in Table 1) reflects the volume of flow over the monitored period and is important because adequate flow is essential for river ecosystem health (Rankin, 1995; Xu and Li, 2016). At each reach section, the ratio of the width of water surface to the width of the river was calculated using UAV orthophotographs. The average of three sections i.e., the sampling site, and 150 m upstream and 150 m downstream of the site - was calculated as the status of channel flow at that particular site.

Channel Sinuosity (Index 4 in Table 1) is an important attribute in many rivers and has a positive effect on medium and long-term river ecosystem health (Brussock and Brown, 1991; Rankin, 1995; Deng et al., 2015). In this study, "Google Earth" data were used to vectorize 20 km of the river channel along the bank line. Sinuosity is defined as the ratio of the length of the river to the straight line. A viewing height of 1 km above the ground in "Google Earth" was used to ensure the image was clear at a moderate scale.

Channel Alteration (Index 5 in Table 1) indicates the degree of channelization. Highly channelized rivers, assigned a low value in this index, impact aquatic habitat and its biota (Barbour et al., 1999; Kim and An, 2015). In this study, the river image was vectorized from the UAV orthophotographs for sections 150 m upstream and downstream of the sample location. The ratio of the length of the river without artificial alteration to the total length of the river was the index score. A value nearly equal to 1.0 suggests a natural river without any alteration.

Bank Stability (Index 6 in Table 1) is an important index for short-term stability of the river. Unstable embankments can lead to problems such as erosion and alteration of channel morphology (Brussock and Brown, 1991; Che et al., 2012; Wang et al., 2016). In this study, the ratio of non-eroded bank length to total vectorized bank length represents bank stability, in which 300-meter-long images of the river bank were vectorized from the UAV orthophotographs. Erosion was identified using the method of Marteau et al. (2017) by comparing two periods of the UAV-retrieved elevation values of bank pixels, where changes >10 cm were considered to be eroded.

Riparian Zone Vegetation Diversity and Coverage (Indices 7 and 8 in Table 1), which represent the riparian vegetation status, have an important positive effect on river ecosystem health, as diversified and dense riparian vegetation protects the bank from erosion, reduces pollutant runoff into the river and provides a diverse habitat for wildlife (Brussock and Brown, 1991; Rankin, 1995; Deng et al., 2015). In this study, we estimated riparian vegetation diversity using 30-m long and 5-m wide transects taken on each bank of the sampling site and, 150-m upstream and downstream of the site. Plant species were identified and the coverage of each species i (s_i) on the transect was estimated. Vegetation diversity (H_V) was calculated using the formula for Index 7 (Table 1). Vegetation coverage was calculated based on the following rules: 1) "g>r & g>b" where r, g, b represents the value of the red, green and blue bands respectively in the orthophotograph; 2) "g > x" where x is the threshold value of the green band (Zhang et al., 2007a, 2007b), which ranged from 30 to 45. Larger values of the two indices imply better river ecosystem health.

Riparian Vegetative Zone Width (Index 9 in Table 1) has a direct influence on the health of rivers, as wider riparian vegetation zones can better prevent pollutant runoff from entering the river (Pariyadath and Eagleman, 2007). In this study, we used UAV orthophotographs to measure the width of the riparian vegetation zone 150 m upstream and downstream of each sampling site and divided this width by 18 since a riparian zone 18-m wide is considered sufficient to protect river banks (Barbour et al., 1999). Larger values of the riparian vegetation zone imply better river condition.

Nonpoint Source Pollution (Index 10 in Table 1) negatively impacts on river ecosystem health in areas with intensive human activities where large amounts of non-point source pollutants enter the river (Powers et al., 2016), which contributes to eutrophication leading to ecosystem degradation (Wei et al., 2009; Che et al., 2012; Deng et al., 2015; Pan et al., 2015). To assess nonpoint source pollution impacts on river ecosystem health, "Google Earth" was used to measure the length of the nonpoint source pollution section along the river bank within 1 km upstream and downstream of the monitoring site, the ratio of which to the total channel length suggests the degree of influence of nonpoint source pollutants. To facilitate this assessment, we used higher values to reflect better conditions, with few nonpoint source pollutants discharging into the river. For details, please refer to the formula in Table 1.

The semi-quantitative indices in the RBPs were converted to quantitative ones. Improving these indices enhances the objectivity of the evaluation results, reduces the dependence on the experience of the evaluators, and more importantly allows more realistic comparison of the results between different regions, e.g., China and the United States.

[1] http://www.esri.com/arcgis
[2] https://www.google.com/earth/

Table 1
Newly developed physical habitat quality assessment methodology based on conceptions in the RBPs (Appendix Table S1). Attributes of geomorphology, hydrology, riparian vegetation and non-point source pollution are quantitatively formulated.

Index	Formula	Description	Position in Appendix Table S1
1. Epifaunal Substrate and Embeddedness	$ESE = \frac{s-1}{\ln N}$	The s is the total area of individuals in the community and N is the total area of individuals observed, details refer to Margalef (1958) and Gamito (2010). The area could be measured from orthophoto imagery. Higher values are considered to indicate better conditions.	Habitat Parameter 1 (Barbour et al., 1999)
2. Velocity & Depth Regime	$\sigma_d^2 = \frac{\sum (dep_i - 0.5)^2}{N}, \sigma_v^2 = \frac{\sum (vel_i - 0.3)^2}{N}$ $VDR = (\sigma_d^{2'} + \sigma_v^{2'})/2$	σ_d^2, σ_v^2represent variances of depth and velocity, respectively;$\sigma_d^{2'}$and$\sigma_v^{2'}$ were normalized variances of depth and velocity. Orthophotographic images are generated by UAV, and a visual judgment standard score is determined from these images. The general guidelines are 0.5 m depth to separate shallow from deep, and 0.3 m/s to separate fast from slow (Barbour et al., 1999).	Habitat Parameter 3 (Barbour et al., 1999)
3. Channel Flow Status	$CFS = \frac{Water\ width}{Channel\ width}$	Water width and channel width are measured from UAV orthophotographic images at each sampling site and 150 m downstream and upstream. An average value is calculated from these measurements. Higher values are considered to indicate better conditions.	Habitat Parameter 5 (Barbour et al., 1999)
4. Channel Sinuosity	$CS = \frac{Channel\ length}{Valley\ length}$	Use Google Earth data to obtain a vectorized 20 km reach along the river channel, CS is the ratio of channel length and the straight distance between the start point and end point of that reach. For CS < 4, higher values indicate better conditions; for CS > 4, lower values indicate better conditions.	Habitat Parameter 7 (Barbour et al., 1999)
5. Channel Alteration	$CA = 1 - \frac{Alteration\ length}{Channel\ length}$	The altered length and channel length are measures from vectorized orthophoto imageries along 300 m of the river channel. Higher values are considered to indicate better conditions.	Habitat Parameter 6 (Barbour et al., 1999)
6. Bank Stability	$BS = 1 - \frac{Unstable\ length}{Channel\ length}$	The unstable length and channel length are measures from vectorized orthophoto imageries along 300 m of the river channel. Higher values are considered to indicate better conditions.	Habitat Parameter 8 (Barbour et al., 1999)
7. Riparian Zone Vegetation Diversity	$RZVD = -\sum (s_i/S_t) \ln (s_i/S_t)$	Use orthophoto maps at each sampling site and 150 m upstream and downstream on the river on both sides to define transects 30-m long and 5-m wide, Plant species were identified by visual discrimination and the area of the species i (s_i) on the graph was delineated. S_t represents the total area of all species. Higher values are considered to indicate better conditions.	Habitat Parameter 9 (Barbour et al., 1999)
8. Riparian Zone Vegetation Coverage	$RZVC = \frac{Vegetation\ coverage\ area}{Total\ area\ of\ demo}$	Use UAV orthophoto imagery at each sampling site and 150 m upstream and downstream to define 30-m long and 5-m wide transects, use the software to calculate the vegetation cover and average the results. Higher values are considered to indicate better conditions.	Habitat Parameter 9 (Barbour et al., 1999)
9. Riparian Zone Vegetation Width	$RZVW = \begin{cases} width/18, & width<18 \\ 1, & width \geq 18 \end{cases}$	Use UAV orthophoto imagery at each sampling site 150 m upstream and downstream, along left and right banks, measure the width of riparian vegetation at each location and average these measurements. Higher values are considered to indicate better conditions.	Habitat Parameter 10. (Barbour et al., 1999)
10. Non-point Source Pollution	$NSP = 1 - \frac{Non-point\ pollution\ length}{Channel\ length}$	Use Google Earth imagery to identify and locate possible non-point sources 1 km upstream and downstream of each sampling site and within 50 m of the river, and calculate the length of reach with possible non-point issues. Higher values are considered to indicate better conditions.	Newly developed in this study.

Indices 1–9 were formulated based on original RBPs; Index 10 was newly developed in this study.

To further quantify the uncertainties of the original RBPs values, we calculated the difference between the RBPs-estimated indices and the UAV orthophotograph derived indices using Eq. (1), using the physical habitat indices as an example.

$$V = (Score_{UAV} - Score_{ori})/Score_{UAV} \quad (1)$$

where V represents the difference between the two methods, with $Score_{UAV}$ representing the score obtained from the UAV orthophotographs and $Score_{ori}$ is the score obtained by the original RBPs.

3.1.2. Using biodiversity to reflect variation in biological communities in river ecosystem health assessment

Biodiversity indices have been widely used to assess aquatic ecosystem health (Keylock, 2005; Pinheiro et al., 2015; Fierro et al., 2017). In this study, the Shannon-Weiner diversity was used to assess the health status of the aquatic community. Generally, in aquatic ecosystems the zoobenthos and fish are often used as indicators of ecosystem health (Liu et al., 2011; Zhao et al., 2018). The zoobenthos is more sensitive than fish to changes in the aquatic environment, but the former often recovers more quickly than the latter after a disturbance. Thus, the diversities of both zoobenthos and fish were used as indices of river ecosystem health to provide an assessment of the short-term and long-term health status of a river.

3.1.3. Selection of water quality indices to reflect the impact of pollution on river ecosystem health

Due to the high correlation and information redundancy among water quality indices, a correlation analysis was used to remove redundant water quality indices. The remaining indices were then used to determine the score for water quality. The Kolmogorov-Smirnov normal distribution test (Smirnov, 1948; Arnold and Emerson, 2011) was performed prior to correlation analysis. Pearson correlation analysis (Pearson, 1895) was used for indices that meet the assumption of normality, and the Spearman rank correlation analysis (Spearman, 1904) was applied to the remaining indices. A correlation coefficient of 0.6 between any two indices was deemed as the threshold value to select independent indices. Normality distribution tests and correlation analyses were conducted using SPSS[3] software.

3.1.4. Integrated assessment of river ecosystem health

The entropy method has been demonstrated to objectively derive the weighting assigned to each index and is widely used in engineering technology, social economy, environmental evaluation and sustainable management (Hao and Singh, 2013; Liu et al., 2014; Zhang et al., 2014; Díaz-Varela et al., 2016). The basic idea behind the entropy method is to determine the weight based on the variability of the

[3] http://www.spss.com.cn/

index. In general, the larger the amount of information provided by the index, the greater the weight in the overall evaluation (Harte and Newman, 2014). In order to objectively determine the weights of the indices, we first need to eliminate the influence of the different dimensions between the indicators. The original indicator data were standardized with Eq. (2).

$$y_{ij} = \frac{x_{ij} - x_{\min}}{x_{\max} - x_{\min}} \tag{2}$$

Second, entropy and entropy weightings can be determined with Eq. (3).

$$H_j = -K \sum_{i=1}^{m} \left(f_{ij} \ln f_{ij} \right) \tag{3}$$

H_j is the entropy of the index j, $f_{ij} = y_{ij} / \sum_{i=1}^{n} y_{ij}$, $k = 1/\ln n$.

We assume that when f_{ij} is zero, $f_{ij} \ln f_{ij}$ equals to zero. And then the weighting of the index j can be calculated with Eq. (4).

$$w_j = \frac{1 - H_j}{\sum_{j=1}^{n} (1 - H_j)} \quad 0 \le w_j \le 1, \sum_{j=1}^{n} w_j = 1 \tag{4}$$

Based on entropy and using quantified biological, water quality and physical habitat indices, the abovementioned river-ecosystem health (RH) was calculated with Eq. (5):

$$\begin{aligned} RH &= \textstyle\sum_{i=1}^{n} w_i \cdot P_i \\ P_i &= \textstyle\sum_{j=1}^{m} w_{ij} P_{ij} \end{aligned} \tag{5}$$

where RH is the integrated health score weighted by its first-level indices (i.e., biological, water quality and habitat status) (Fig. 2), and a higher RH value implies a healthier river ecosystem condition. i and j denote the i-th and j-th indices, respectively; n and m are the total number of first and second level indices, respectively; P_i, wi, P_{ij} and w_{ij} represent the first-level index, first-level index weight, second-level index, and second-level index weight, respectively.

3.2. Data

To explore the health of the river system in the Jinan catchment, six extensive field campaigns were conducted to monitor the nominated river attributes (May-2014 (spring), Aug-2014 (summer), Nov-2014 (autumn), May-2015 (spring), June-2015 (summer), Oct-2015 (autumn)). Information on instream biota, water quality, and physical habitat were collected in situ using portable equipment in each field campaign. The length of the river sections sampled was 300 m

Zoobenthos and fish were collected and preserved in 10% formalin solution, and were classified and weighed in the laboratory. Details on the collection methods are as follows.

3.2.1. Zoobenthos

In mountain streams with depths <30 cm or the shallow zones of rivers, a Sürber sampler (0.5 × 0.5 m) with a 60 μm mesh size net was used to collect samples. For deep biotopes, a 1/16 m^2 Peterson grab sampler was used to collect samples. A 60 μm mesh size screen was used to rinse the collected bottom mud, and all retained material was poured into a white ceramic plate and all animals were handpick, stored in a 1-L-wide-mouth bottle and preserved with 70% alcohol.

3.2.2. Fish

For wadable rivers with depths <1.5 m, an electric fishing apparatus was used to sample fish. The sampling process involved one operator using a 20-pipe ultrasonic electric fishing apparatus to catch the fish, while another operator collected samples with a dip net. The samples were collected under different flow velocity and depth conditions. The sampling period was 30–60 min. For non-wadable rivers with depths >1.5 m, a boat was used to catch the fish by trawling over a distance not exceeding 100 m between each sampling point. Fish were also collected from fishermen (if available).

In total, 73 species of benthic organisms (belonging to 3 phyla, 6 classes, 12 orders, 26 families) and 58 species of fish (belonging to 1 phylum, 1 class, 7 orders, 19 families) were recorded.

Water quality parameters were also measured in situ, and water samples for chemical analysis were concurrently collected at the monitoring sites and tested in the laboratory within 24 h following the methods of the national environmental quality standards for surface water "GB 3838-2002" (Zhao et al., 2018). Dissolved oxygen (DO) and pH were measured using a portable HACH kit (PC101). An ion chromatograph (DIONEX-600) was used to measure fluoride (F), sulfate (SO_4^{2-}), chloride (Cl^-) and nitrate (NO_3) concentrations; a spectrophotometer (DR5000) was used to measure total nitrogen (TN), ammonium nitrogen (NH_4-N), total phosphorus (TP) and hexavalent chromium; and an automatic Flow Injection Analyzer (KALAR SAN++) was used to measure volatile phenols (VP), anionic detergents (AS). In total, 36 water quality parameters were analyzed (see Table 2).

Physical habitat information included **(a)** 381 physical habitat scores that were estimated across sites using the original RBPs (Barbour et al., 1999) over the six field campaigns. They were used to study uncertainties compared with that of UAV orthophotographic observations. The physical habitat status was assessed semi-quantitatively using ten attributes covering four grades (optimal, suboptimal, marginal, and poor), and **(b)** 9551 RGB UAV orthophotographs taken by a DJI Phantom 3 Pro drone with Pix4D control software. Image overlap was set to 90%, and flight height was generally set at 100 m. Post-processing of images was performed using Pix4D Mapper[4] software, with an average ground sampling distance (GSD) under 5 cm. Geographical coordinates were WGS84, and projected coordinates were WGS84/UTM zone 50 N. More details are

Table 2
Water quality data in Jinan City over the six field campaigns from 2014 to 2015.

NO.	Parameter	Abbreviation	Range	SD
1	Ammonia nitrogen	NH_4-N	0.03–75.80	4.85
2	Anion Surface	AS	0–3.48	0.34
3	Bicarbonate	HCO_3^-	0–2247	149
4	Biochemical Oxygen Demand	BOD	0–57.50	4.83
5	Calcium	Ca^{2+}	0.99–486	56
6	Carbonate	CO_3^{2-}	0–38.50	4.93
7	Chemical Oxygen Demand	COD_Cr	0–275	23.74
8	Chlorine	Cl^-	0.99–1156	165
9	Conductivity	Cond	287–57,756	852
10	Dissolved Oxygen	DO	0–13.50	2.25
11	Fluoride	F	0.18–2.51	0.34
12	Natrium	Na^+	0–109	7.9
13	Nitrate	NO3-N	0–22.00	3.34
14	Nitrite	NO2-N	0–1.97	0.25
15	Permanganate index	COD_Mn	0.57–71.50	5.84
16	pH	pH	6.90–9.30	0.39
17	Potassium	K^+	0–767	117
18	Sulfate	SO_4^{2-}	0–1046	170
19	Sulfide	S	0–1.29	0.11
20	Total Alkalinity	TA	0.99–1057	87
21	Total Hardness	TH	0.99–1400	222
22	Total Nitrogen	TN	0.25–80.03	6.07
23	Total Phosphorus	TP	0–8.06	0.68
24	Turbidity	Turb	0.52–924	103
25	Volatile Phenol	VP	0–0.16	0.22

a. Cyanide and the other 10 heavy metal ions, e.g., copper, zinc, lead, were below detection and they are therefore omitted.
b. All units except for Turb (deg), pH and Cond (mS/m) of the chemical attributes are in mg/L.

[4] https://pix4d.com

provided in Zhao et al. (2017). **(c)** One satellite image of the study area was taken from Google Earth on 31/12/2016 with a view height set to 1 km.

4. Results

4.1. Physical habitat indices calculated with newly developed quantitative methodologies

Based on the formulae in Table 1, the physical habitat indices were calculated as shown in Table 3.

The results in Table 3 show that the river habitat was spatially heterogeneous: the habitat average scores at J1, J5, J16, and J32 were 0.59, 0.62, 0.61, and 0.49, respectively. J5 scored the highest, as it is a completely natural river bank with the densest coverage and widest band of riparian vegetation; J32 scored the lowest due to its poor flow condition. In addition, J5 had the highest second-level index scores for riparian vegetation coverage (0.83) and width (0.74), as well as higher scores for eight other second-level indices which further supported its superior stream condition compared with the other three sites. In contrast, the lowest second-level index scores for velocity and depth regime (0.15), channel flow status (0.15) and nonpoint source pollutants (0.11) reduced the total score of J32.

Compared with previous empirical scoring methods, where most of the distance or area-related indices were visually estimated rather than measured (e.g., Velocity and Depth Regime, Channel Sinuosity, Channel Alteration, and Riparian Zone Vegetation Diversity in original RBPs), UAV orthophotographic imagery provides a convenient and accurate method for long-distance and large-area measurements (Chen et al., 2017; Qayyum et al., 2017). Thus, this method was used to calculate distance or area related physical habitat indices (Table 1). The calculated index values were compared with that of the original RBPs values from the four representative sites (J1, J5, J16, and J32) as shown in Fig. 3. Six of the ten indices were different (Fig. 3). Specifically for bank stability and channel alteration (thick circles in Fig. 3), the values estimated by the original RBPs differed statistically from those calculated by the UAV orthophotographic method; the latter method undoubtedly providing a better evaluation of these indices.

Based on absolute values of V, we found that of the 59 sampling records, 39 records had $Score_{ori}$ values greater than zero due to errors in estimating distances. The percentage error exceeded 10% in nearly 80% (31/39) of the records, illustrating that the majority of values estimated by the RBPs were not as accurate as the UAV orthophotographic values; for 25% (10/39) of the records, the percentage error estimated by the RBPs exceeded 50%; and for 13% (5/39) of the records, the percentage error exceeded 70%, suggesting that quite a number of the estimates of the RBPs deviated substantially from their true values, as shown in Appendix Fig. 1. The comparison between the RBPs-estimated and the UAV-orthophotographic indices suggests that the former indices contained large errors. This indicates that the UAV orthophotographic imagery method does greatly improve the accuracy and stability of index assessment.

Table 3
Habitat condition in the four representative key sites (J1, J5, J16, and J32).

Indices	J1	J5	J16	J32	Average
Epifaunal Substrate and Embeddedness	0.80	0.35	0.25	0.50	0.48
Velocity & Depth Regime	0.80	0.65	0.25	0.15	0.46
Channel Flow Status	0.80	0.65	0.25	0.15	0.46
Channel Sinuosity	0.34	0.28	0.31	0.29	0.31
channel alteration	0.00	1.00	1.00	1.00	0.75
Bank Stability	1.00	0.91	0.93	1.00	0.96
Riparian vegetation diversity	0.51	0.51	0.74	0.65	0.60
Riparian vegetation coverage	0.53	0.83	0.79	0.61	0.69
Riparian vegetation width	0.38	0.74	0.53	0.47	0.53
Non-point pollutants	0.77	0.25	1.00	0.11	0.53
Average	0.59	0.62	0.61	0.49	0.58

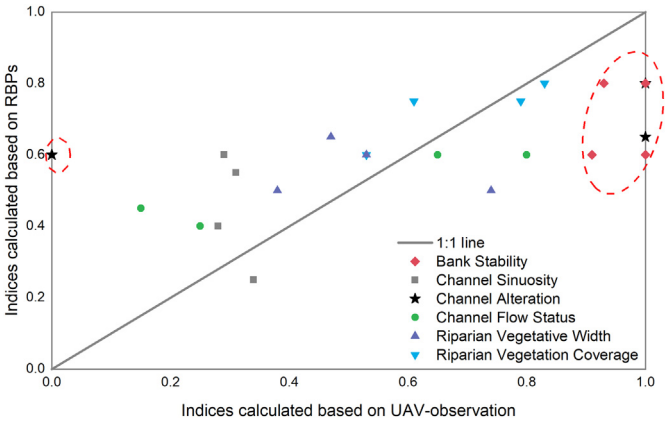

Fig. 3. Comparison of results calculated by the two methods. The horizontal axis represents indices calculated using the new UAV orthophotographic method, and the vertical axis represents indices estimated by the RBPs.

4.2. Biological variation indicated by diversity

Sampling sites J1, J5, J16, and J32 are located in key riverine reaches targeted for ecological remediation (see Fig. 1 for sampling locations); thus their ecological condition has been monitored over time. The biological data obtained from these sites are shown in Appendix Fig.S2. The maximum diversity value was 2.98, while the minimum was 0.88 with a mean of 1.98 for the zoobenthos. For fish, the maximum diversity was 3.62, while the minimum was 1.37, with a mean of 2.41. In general, fish diversity was higher than that of the zoobenthos (Appendix Fig.S2).

4.3. Selection of water quality indices for river ecosystem health assessment

Correlation analysis showed that the correlation coefficient between pH and carbonate was 0.61 ($p < 0.01$). However, pH had higher average correlation coefficients with the remaining attributes than that with carbonate (Appendix Fig.S3); as such pH was retained, and carbonate was deemed redundant. Chloride was highly correlated with conductivity, sulfate, bicarbonate, potassium permanganate index, total hardness, total alkalinity, fluoride, Na, and K (correlation coefficients ranged from 0.61 to 0.94 with $p < 0.01$), so chloride was retained, and the other indices were deemed redundant. Similarly, Turb, pH, Ca, Cl, DO, TN, NH_3-N, NO_2-N, COD, and BOD were selected and retained in determining the water quality indices.

4.4. River ecosystem health assessment

After selecting the biological, water-quality and habitat indices, the health of the river in the study area was assessed using Eq. (5). The weight of each index was calculated using the entropy method (Eqs. (2)–(4), in Appendix Table S2). An index with little variance was automatically assigned a low weight value, and vice versa. The weights of the three first-level indices were 0.29 (biological status), 0.64 (water quality status) and 0.07 (habitat status), which indicates that habitat status in the study area (in Appendix Table S2), e.g., channel sinuosity and bank stability, varied less than that for water quality. Among the three first-level indices, the smaller the water quality index value, the higher the quality of water, while the reverse was true for the other two first-level indices. Consequently, the reciprocal of water quality attributes was used for assessing the health of the river. For the secondary biological indices, the weights of the diversity of the zoobenthos and fish were 0.66 and 0.34, respectively, while the maximum weight for water quality was 0.31 for ammonia and the minimum weight was

0.01 for pH, respectively. For the secondary indices of physical habitat, the maximum weight was 0.31 for river channel alteration, and the minimum was 0.01 for bank stability.

Using these weights the health status of the river in the study area was calculated using Eq. (5), as shown in Fig. 4. Its health status showed different characteristics, with four different trends over a year.

- Increasing trend (Fig. 4a) in mountainous rivers with minimal human activity: the key driving attributes were turbidity and total nitrogen concentrations, which generally decreased throughout the year. An increasing trend for turbidity and total nitrogen occurred in a mountainous river also with a little human activity, where high river flows dilute the concentration of pollutants in summer and autumn, especially in the former, resulting in better water quality status (Wang et al., 2017), as shown at J1.
- Parabolic trend (Fig. 4b) in mountainous rivers with intensive human activity: the river ecosystem health status was best in summer and lower in spring and autumn because the upstream reservoir retained water in spring and autumn to meet the demand for water for anthropogenic activities. This, coupled with substantially less rainfall and higher pollutant concentrations than that in summer, resulted in poor water quality in the downstream reaches which seriously impacted the health of the river ecosystem (Chen et al., 2005), as indicated at J5.
- Falling trend (Fig. 4c) in river plains mostly occupied by farmland: river ecosystem health was good in spring, but the score dropped markedly in summer and autumn as exemplified at site J16. This was due to the fact that there are many sluices/weirs and dams in this catchment resulting in frequent zero flows in summer and autumn, while in spring, the demand for irrigation water to service agricultural activities maintained the flow of water in the rivers (Zhao et al., 2015). The change in river flow influenced zoobenthic and fish diversities, chemical oxygen demand, biological oxygen demand, total nitrogen and ammonia nitrogen, leading to seasonal variations in the health status of the river.
- Decreasing trend (Fig. 4d) in river plains with sparse farmland: the river ecosystem health score decreased slightly from spring to autumn as exemplified by site J32. The key attributes influencing the trend were zoobenthic and fish diversities. In a river plain with little agricultural influence water quality varied negligibly (Zheng and Lv, 2016). As such, the variations in biological status over seasons drove the trend in river ecosystem health. This was especially due to variations in zoobenthic diversity (with values of 1.71 through 0 in the first year and 2.67 through 1.71 in the second year).

Overall, changes in river ecosystem health in the study area were principally driven by variations in the biological status and water quality, as these variations were far greater than those of the habitat (Fig. 2). The river ecosystem health scores showed that it was best over summer (0.65), followed by spring (0.62), and poorest in autumn (0.40). Specifically, the health status of mountain rivers (J1 and J5) was better than that in the remote plains (J32), while it was worst in the city (J16). Because J1 is located upstream of a reservoir and J5 is downstream, the water captured in the reservoir led to lower river flow downstream, resulting in a decrease in biodiversity at J5, and its lower score relative to J1. The health status of the river at both mountain sites (J1 and J5) improved significantly from spring to summer. However, J16, located in the city, had a poor overall status, as flows were low or absent in summer and autumn over the two-year sampling period. During spring and autumn, biological diversity decreased gradually, which negatively affected the final river ecosystem health score at J32.

An index with a higher score suggests greater river ecosystem health, as shown in Appendix Fig. S4. The score of first-level indices (water quality (WQ), physical habitat (HQ), and biological (BIO)

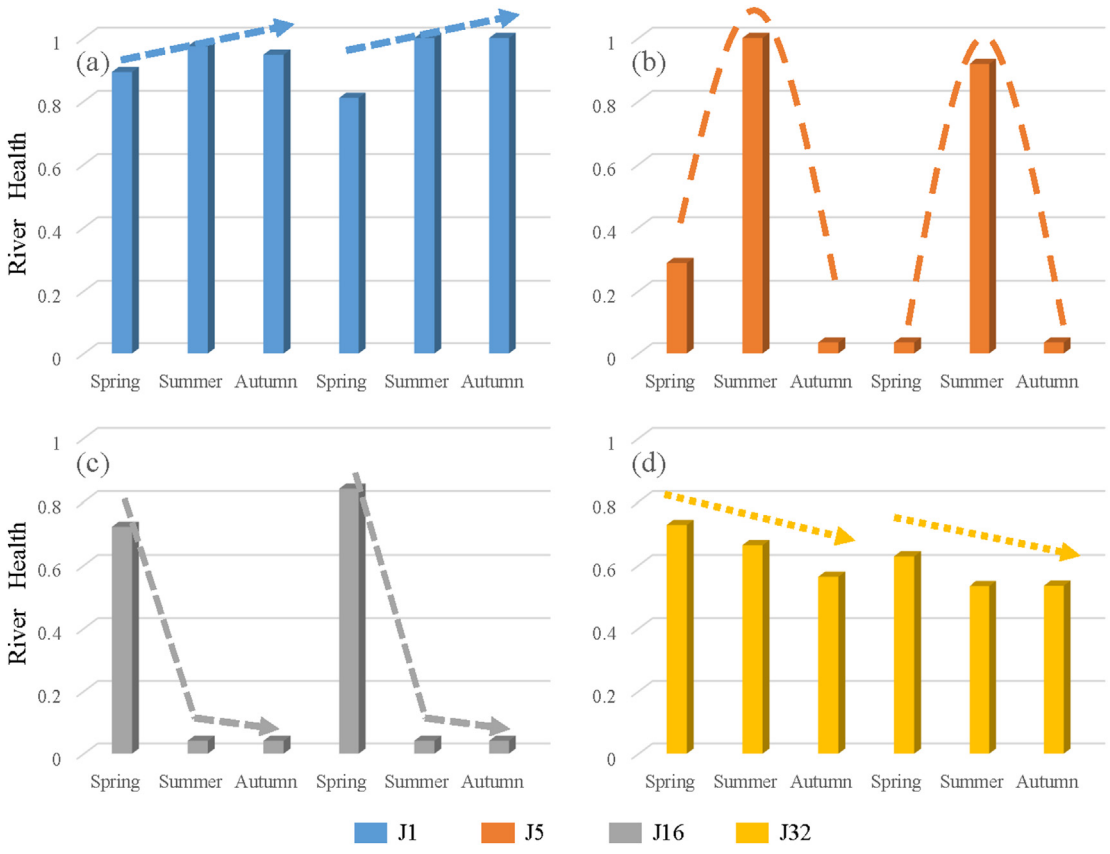

Fig. 4. River ecosystem health at the four representative sites of J1 with increasing trend (a), J5 with parabolic trend (b), J16 with falling trend (c) and J32 with decreasing trend (d).

attributes) showed that water quality played an important role in assessing river ecosystem health. Over the six sampling events from May 2014 to October 2015, WQ contributed significantly more to the health of river than BIO and HQ attributes.

5. Discussion

5.1. Improved accuracy for assessing the physical habitat quality using low-altitude UAV orthophotographic imagery

The use of UAV orthophotographic imagery greatly improved the accuracy of habitat ratings, as it overcame the shortcomings of subjective estimations of distance and area used in traditional methods, which often introduced large errors and reduced assessment accuracy (Stockdale et al., 2015). Experiments by Levin and Haber (1993) showed that humans typically incur a ± 10% error in estimating distances, which increases with distance. Also, error estimating the size of distant objects increases with distance due to visual illusion (Pariyadath and Eagleman, 2007; Zhou et al., 2013; Van der Hoort and Ehrsson, 2016). The effects of visual illusion in estimating river habitat attributes can be significant, especially when estimating water surface width, channel width, channel alteration, and width of the riparian vegetation zone, leading to substantial assessment errors. This problem is less likely to occur using UAV orthophotographic imagery, and measurement errors tend to be very small (Harwin et al., 2015) as the attributes can be quantitatively measured on these images (Appendix Fig. S5), thus providing a more accurate assessment of habitat conditions.

To further explore the errors incurred in estimating distances the channel flow index (Index 3, Table 1) was selected to assess the effect distance perception error would have on assessing river ecosystem health. Channel flow status was calculated using the equation in Table 1. Both channel width and water surface width were measured on the orthophotographs. Most previous studies determining the score of this index used visual estimation of distances. For example, with an error of approximately ±10% in visually estimating distances a true value of 44.22 m may be estimated as 10% less than this value, i.e., 39.80 m, or 10% more than the true value, i.e., 48.64 m, as shown in Appendix Fig.S5.

With a ±10% error in estimating distances, the score of the channel flow status index (Index 3, Table 1) will vary from 0.82 to 1.22 times its true value. At the four sampling sites J1, J5, J16, and J32, the index scores were 0.59–0.89, 0.60–0.90, 0.35–0.52, 0.69–1.00, respectively (Appendix Table S3), which translates to an error range of 18%–22%. In short, errors emanating from visual estimations usually result in large uncertainties depending on its geographical surroundings.

Since the effects of visual distance estimation errors cascade through the habitat evaluation process, these errors will ultimately affect the accuracy in assessing river ecosystem health. Because each error is a function of many factors, including angular declination below the horizon, eye height, and intrinsic bias, it is difficult to distinguish between systematic error and random error and therefore difficult to adjust for this error. This scenario results in considerable randomness and instability in the evaluation outputs, and therefore reduces its ability to compare the health of rivers across different periods and regions.

These shortcomings were overcome using the UAV orthophotographic imagery method with known geographical coordinates, and the plane precision after adjustment was <0.05 m, allowing measurement of distance or area directly from the photographs using ArcGIS or AutoCAD. This allowed more precise comparisons between different periods and regions.

5.2. Weight calculation and its influencing factors

In Section 4.4, the weights for biological, water quality and physical habitat indices were calculated to be 0.29, 0.64 and 0.07, respectively.

Table 4
Descriptive statistics of aquatic biota, water quality and habitat quality.

	Maximum	Means	SD	Variance	Skewness		Kurtosis	
	SQ	SQ	SQ	SQ	SQ	SE	SQ	SE
BIO	3.03	1.96	0.83	0.69	−0.92	0.55	0.46	1.06
WQ	30.44	11.95	7.81	60.99	0.96	0.55	0.5	1.06
HQ	0.73	0.58	0.10	0.01	0.33	0.47	−1.44	0.92

SQ: statistical quantity; SE: standard error. BIO: aquatic biota; WQ: water quality; HQ: habitat quality.

The weight for the water quality index significantly exceeded the other two indices, with the weight for the physical habitat index being less than one-tenth that of the water quality index. Previous studies have shown that water quality is important to river ecosystem health (Mouton et al., 2012; Palmer et al., 2014), which is consistent with our study, where water quality status varied widely and thus had the greatest weight value, while physical habitat status was less variable, with the smallest weight value as determined by the entropy method.

The entropy method is based on information entropy in which an index with greater variance is assigned greater weight (Zhao et al., 2012). In this study, the water quality attributes varied widely spatially and temporally; thus, it was assigned a greater weight value. To illustrate these variations, we used two scenarios to consider the impact of index variations on weightings: first, to randomly alter the second-level water quality indices around the maximum index values (i.e., extremely polluted water) within the range of ±10–50%, and keeping those of biology and habitat unchanged (Table 4 and Appendix Table S2) (as shown in the left sub-figure in Appendix Fig.S6); and second, to randomly alter these indices around their minimum values (i.e., cleanest water) within different ranges, with those of biology and habitat unchanged (right sub-figure in Appendix Fig.S6).

We found that when the water quality indices varied within ±10% of the maximum (i.e., poorest water quality), the weights of water quality varied between 0.02 and 0.05, and the weights for the biological and habitat indices varied between 0.8 and 0.15; when the water quality indices varied within ±10% of the minimum, the result was close to that of the above (Appendix Fig.S6). The degree of water quality (polluted or clean) does not influence the magnitude of the weighting. However, if the range of variation of water quality gradually increased (from 10% to 50%), the weight increased rapidly, and weights for the biological and physical habitat indices decreased steeply; when the water quality variation was 50%, the weight of the biological index decreased to approximately 0.5, and that of the habitat index decreased to approximately 0.1. Thus, the weight of the water quality index was mainly determined by the variability of the data. In other words, an index with great variability is automatically assigned a large weight value.

5.3. High spatial resolution UAV orthophotographic imagery to improve the accuracy calculating an index

To illustrate the influence of imagery resolution on the results, UAV orthophotographs were taken at different flight heights with resolutions of 5 cm × 5 cm, 10 cm × 10 cm, 20 cm × 20 cm, and 40 cm × 40 cm and calculated vegetation coverages of 98.78%, 99.21%, 99.65%, and 100%, respectively.

For dense vegetation coverage and low resolution, the low proportion of water surface was misidentified as vegetation, resulting in a calculated vegetation coverage that was higher than the actual value. In contrast, if vegetation coverage and resolution were both low, then the low proportion of vegetation area was misidentified as water surface, resulting in a calculated vegetation coverage much lower than the actual value.

The lower image resolution led to greater difficulty in identifying types of vegetation and therefore erroneously low values of biodiversity.

High-resolution images (e.g., a resolution of 5 cm × 5 cm used in this study) improved recognition of vegetation types, accuracy of vegetation diversity, and vegetation coverage calculations.

6. Conclusions

To overcome the shortcomings of subjectivity and the lack of quantification and comparability in previous river ecosystem health assessment studies, we developed an assessment methodology using UAV orthophotographs to calculate the physical habitat indices, which was then applied to assess the health of rivers. Twenty-two indices were used to determine the status of the biological, water quality and habitat components. Mountain rivers had the best health status with a score of 0.94; and temporally the health condition of rivers was best in the summer with an average score of 0.65, while it was poorest in autumn with a score of 0.40. Changes in the health of rivers in this study area were driven by variations in the status of the biological and water quality components instead of that of the physical habitat. In determining the weights of each attribute, an index with great variability was automatically assigned a large weight value. We found that values estimated by the original RBPs differed greatly from those calculated using the new UAV orthophotographic image-based method. The RBPs-estimated indices produced large errors compared to that of the UAV orthophotographic indices. Uncertainties (approximately 20%) in estimating distances and heights visually and subjectively by observers greatly reduced the assessment accuracy of the former method, resulting in randomness and instability, thus reducing comparability of results across different periods and regions. This was largely overcome by using the new quantitative methodology presented in this study. This new methodology improved the assessment of river health by accurately measuring and objectively weighting the physical habitat indices, making it amenable to assessing a variety of river conditions across the globe.

While this new methodology was developed with comparatively short-term datasets with some attendant uncertainties in their outputs, long-term monitoring datasets should reduce these uncertainties.

Statement of authorship

ZC, DT and LC designed the study; ZY performed modelling work and analyzed output data; GY, YX and ZY collected data and performed the meta-analysis; ZC, PT, LJ, MS, LR and ZY wrote and revised the manuscript.

Acknowledgments

We would like to thank Professor Margaret Palmer from the University of Maryland for her insightful ideas on aquatic ecosystem restoration and services. We acknowledge the reviewers and editors for their valuable advice on improving the quality of this paper. We thank the China Scholar Council (CSC) and our colleagues from Dalian Ocean University, Jinan and Dongying Survey Bureau of Hydrology, and Beijing Normal University for their support in funding this research and collaboration during field investigations.

This research was jointly supported by the National Natural Science Foundation Program of China (grant numbers u1812401 & 41471340), the 111 Project (B18006), the National Key Project for R&D (grant numbers 2016YFC0402403 & 2016YFC0402409), and the Program for Key Science and Technology Innovation Team in Shaanxi province (grant number 2014KCT-27), China.

Appendix A. Supplementary data

Supplementary data to this article can be found online at https://doi.org/10.1016/j.scitotenv.2019.02.379.

References

Acreman, M.C., Dunbar, M.J., 2004. Defining environmental river flow requirements? A review. Hydrol. Earth Syst. Sci. Discuss. 8 (5), 861–876.
Arnold, T.B., Emerson, J.W., 2011. Nonparametric goodness-of-fit tests for discrete null distributions. R Journal 3 (2), 34–39.
Barbour, M.T., Gerritsen, J., Snyder, B.D., Stribling, J.B., 1999. Rapid Bioassessment Protocols for Use in Streams and Wadeable Rivers. USEPA, Washington.
Blue, B., 2018. What's wrong with healthy rivers? Promise and practice in the search for a guiding ideal for freshwater management. Prog. Phys. Geogr. Earth Environ. 42 (4), 462–477.
Boulton, A.J., 1999. An overview of river health assessment: philosophies, practice, problems and prognosis. Freshw. Biol. 41 (2), 469–479.
Brussock, P.P., Brown, A.V., 1991. Riffle-pool geomorphology disrupts longitudinal patterns of stream benthos. Hydrobiologia 220 (2), 109–117.
Cairns Jr., J., McCormick, P.V., 1992. Developing an ecosystem-based capability for ecological risk assessments. Environmental Professional 14 (3), 186–196.
Cairns, J., McCormick, P.V., Niederlehner, B.R., 1993. A proposed framework for developing indicators of ecosystem health. Hydrobiologia 263 (1), 1–44.
Carbonneau, P.E., Piégay, H., Carbonneau, P.E., Piégay, H., 2012. Fluvial Remote Sensing for Science and Management. John Wiley & Sons.
Che, Y., Yang, K., Wu, E., Shang, Z., Xiang, W., 2012. Assessing the health of an urban stream: a case study of Suzhou Creek in Shanghai, China. Environ. Monit. Assess. 184 (12), 7425–7438.
Chen, J., Wang, F., Meybeck, M., He, D., Xia, X., Zhang, L., 2005. Spatial and temporal analysis of water chemistry records (1958–2000) in the Huanghe (Yellow River) basin. Glob. Biogeochem. Cycles 19 (3), 2299–2310.
Chen, S., Mcdermid, G., Castilla, G., Linke, J., 2017. Measuring vegetation height in linear disturbances in the boreal forest with uav photogrammetry. Remote Sens. 9 (12), 1257–1269.
Clarke, R. T., & Hering, D. (2006). Errors and uncertainty in bioassessment methods—major results and conclusions from the STAR project and their application using STARBUGS. In The Ecological Status of European Rivers: Evaluation and Intercalibration of Assessment Methods (pp. 433-439). Springer Netherlands.
Clarke, R.T., Furse, M.T., Wright, J.F., Moss, D., 1996. Derivation of a biological quality index for river sites: comparison of the observed with the expected fauna. J. Appl. Stat. 23 (2–3), 311–332.
Costanza, R., d'Arge, R., De Groot, R., Farber, S., Grasso, M., Hannon, B., ... & Raskin, R. G. (1997). The value of the world's ecosystem services and natural capital. nature, 387 (6630), 253.
Cui, B., Wang, C., Tao, W., You, Z., 2009. River channel network design for drought and flood control: a case study of Xiaoqinghe River basin, Jinan City, China. J. Environ. Manag. 90 (11), 3675–3686.
Deng, X., Xu, Y., Han, L., Yu, Z., Yang, M., Pan, G., 2015. Assessment of river health based on an improved entropy-based fuzzy matter-element model in the Taihu Plain, China. Ecol. Indic. 57, 85–95.
Díaz-Varela, E., Roces-Díaz, J.V., Álvarez-Álvarez, P., 2016. Detection of landscape heterogeneity at multiple scales: use of the quadratic entropy index. Landsc. Urban Plan. 153, 149–159.
Dufour, S., Bernez, I., Betbeder, J., Corgne, S., Hubert-Moy, L., Nabucet, J., ... Trollé, C., 2013. Monitoring restored riparian vegetation: how can recent developments in remote sensing sciences help? Knowl. Manag. Aquat. Ecosyst. 410, 10.
Dunford, R. , Michel, K. , Gagnage, M. , Piégay, H., & Trémelo, M.-L. (2009). Potential and constraints of unmanned aerial vehicle technology for the characterization of Mediterranean riparian forest. International Journal of Remote Sensing,30(19), 4915-4935.
Fendorf, S., Michael, H.A., van Geen, A., 2010. Spatial and temporal variations of groundwater arsenic in South and Southeast Asia. Science 328 (5982), 1123–1127.
Fierro, P., Bertrán, C., Tapia, J., Hauenstein, E., Peña-Cortés, F., Vergara, C., ... Vargas-Chacoff, L., 2017. Effects of local land-use on riparian vegetation, water quality, and the functional organization of macroinvertebrate assemblages. Sci. Total Environ. 609, 724–734.
Gamito, S., 2010. Caution is needed when applying Margalef diversity index. Ecol. Indic. 10 (2), 550–551.
Grafton, R.Q., Pittock, J., Davis, R., Williams, J., Fu, G., Warburton, M., ... Connell, D., 2013. Global insights into water resources, climate change and governance. Nat. Clim. Chang. 3 (4), 315.
Hankin, D.G., Reeves, G.H., 1988. Estimating total fish abundance and total habitat area in small streams based on visual estimation methods. Can. J. Fish. Aquat. Sci. 45 (5), 834–844.
Hao, Z., Singh, V.P., 2013. Modeling multisite streamflow dependence with maximum entropy copula. Water Resour. Res. 49 (10), 7139–7143.
Harte, J., Newman, E.A., 2014. Maximum information entropy: a foundation for ecological theory. Trends Ecol. Evol. 29 (7), 384–389.
Harwin, S., Lucieer, A., Osborn, J., 2015. The impact of the calibration method on the accuracy of point clouds derived using unmanned aerial vehicle multi-view stereopsis. Remote Sens. 7 (9), 11933–11953.
Hong, Q., Meng, Q., Wang, P., Wang, H., Liu, R., 2010. Regional aquatic ecological security assessment in Jinan, China. Aquat. Ecosyst. Health Manag. 13 (3), 319–327.
Hughes, R. M., Paulsen, S. G., & Stoddard, J. L. (2000). EMAP-surface waters: a multiassemblage, probability survey of ecological integrity in the USA. In Assessing the Ecological Integrity of Running waters (pp. 429-443). Springer Netherlands.
Hughes, R.M., Herlihy, A.T., Kaufmann, P.R., 2010. An evaluation of qualitative indexes of physical habitat applied to agricultural streams in ten US states 1. J. Am. Water Resour. Assoc. 46 (4), 792–806.
Keylock, C.J., 2005. Simpson diversity and the Shannon–Wiener index as special cases of a generalized entropy. Oikos 109 (1), 203–207.

Kim, J.Y., An, K.G., 2015. Integrated ecological river health assessments, based on water chemistry, physical habitat quality and biological integrity. Water 7 (11), 6378–6403.
Levin, C.A., Haber, R.N., 1993. Visual angle as a determinant of perceived interobject distance. Atten. Percept. Psychophys. 54 (2), 250–259.
Liu, C., Zhao, C., Xia, J., Sun, C., Wang, R., Liu, T., 2011. An instream ecological flow method for data-scarce regulated rivers. J. Hydrol. 398 (1), 17–25.
Liu, Z., Han, Z., Zhang, Y., Zhang, Q., 2014. Multiwavelet packet entropy and its application in transmission line fault recognition and classification. IEEE Trans. Neural Netw. Learn. Syst. 25 (11), 2043–2052.
Luo, Y., Ficklin, D.L., Liu, X., Zhang, M., 2013. Assessment of climate change impacts on hydrology and water quality with a watershed modeling approach. Sci. Total Environ. 450, 72–82.
Margalef, R., 1958. Information theory in ecology. Gen. Syst. 3, 36–71.
Marteau, B., Vericat, D., Gibbins, C., Batalla, R.J., Green, D.R., 2017. Application of structure-from-motion photogrammetry to river restoration. Earth Surf. Process. Landf. 42 (3), 503–515.
Marzin, A., Delaigue, O., Logez, M., Belliard, J., Pont, D., 2014. Uncertainty associated with river health assessment in a varying environment: the case of a predictive fish-based index in France. Ecol. Indic. Indices 43, 195–204.
Messinger, M., Asner, G.P., Silman, M., 2016. Rapid assessments of Amazon forest structure and biomass using small unmanned aerial systems. Remote Sens. 8 (8), 615–628.
Meyer, J.L., 1997. Stream health: incorporating the human dimension to advance stream ecology. J. N. Am. Benthol. Soc. 16 (2), 439–447.
Mouton, A.M., Buysse, D., Stevens, M., Van den Neucker, T., Coeck, J., 2012. Evaluation of riparian habitat restoration in a lowland river. River Res. Appl. 28 (7), 845–857.
O'Brien, A., Townsend, K., Hale, R., Sharley, D., Pettigrove, V., 2016. How is ecosystem health defined and measured? A critical review of freshwater and estuarine studies. Ecol. Indic. 69, 722–729.
Palmer, M.A., 2010. Water resources: beyond infrastructure. Nature 467 (7315), 534–535.
Palmer, M.A., Febria, C.M., 2012. The heartbeat of ecosystems. Science 336 (6087), 1393–1394.
Palmer, M.A., Hondula, K.L., Koch, B.J., 2014. Ecological restoration of streams and rivers: shifting strategies and shifting goals. Annu. Rev. Ecol. Evol. Syst. 45, 247–269.
Pan, G., Xu, Y., Yu, Z., Song, S., Zhang, Y., 2015. Analysis of river health variation under the background of urbanization based on entropy weight and matter-element model: a case study in Huzhou City in the Yangtze River Delta, China. Environ. Res. 139, 31–35.
Pariyadath, V., Eagleman, D., 2007. The effect of predictability on subjective duration. PLoS One 2 (11), e1264–e1270.
Pearson, K. (1895). Note on regression and inheritance in the case of two parents. Proceedings of the Royal Society of London, 58, 240-242.
Peng, J., Liu, Y., Wu, J., Lv, H., Hu, X., 2015. Linking ecosystem services and landscape patterns to assess urban ecosystem health: a case study in Shenzhen City, China. Landsc. Urban Plan. 143, 56–68.
Pinheiro, H.T., Di Dario, F., Gerhardinger, L.C., de Melo, M.R., de Moura, R.L., Reis, R.E., ... Rocha, L.A., 2015. Brazilian aquatic biodiversity in peril. Science 350 (6264), 1043–1044.
Plafkin, J. L., Barbour, M. T., Porter, K. D., Gross, S. K., & Hughes, R. M. (1989). Rapid bioassessment protocols for use in streams and rivers: benthic macroinvertebrates and fish. In Rapid bioassessment protocols for use in streams and rivers: Benthic macroinvertebrates and fish. EPA.
Poff, N.L., Brown, C.M., Grantham, T.E., Matthews, J.H., Palmer, M.A., Spence, C.M., ... Baeza, A., 2016. Sustainable water management under future uncertainty with eco-engineering decision scaling. Nat. Clim. Chang. 6 (1), 25–34.
Powers, S.M., Bruulsema, T.W., Burt, T.P., Chan, N.I., Elser, J.J., Haygarth, P.M., ... Sharpley, A.N., 2016. Long-term accumulation and transport of anthropogenic phosphorus in three river basins. Nat. Geosci. 9 (5), 353–356.
Qayyum, A., Malik, A.S., Saad, N.M., Abdullah, M.F.B., Iqbal, M., Rasheed, W., et al., 2017. Measuring height of high-voltage transmission poles using unmanned aerial vehicle imagery. J. Photopolym. Sci. Technol. 65 (3), 137–150.
Rankin, E. T. (1989). The qualitative habitat evaluation index (qhei): Rationale, methods. and application. Technical report, Ecological Assessment Section Division of Water Quality Planning and Assessment, Ohio EPA.
Rankin, E. T. (1995). Habitat indices in water resource quality assessments. Biological Assessment and Criteria*: Tools for Water Resource Planning and Decision Making.* CRC Press, Boca Raton, FL, 181–208.
Rankin, E.T., 2006. Methods for Assessing Habitat in Flowing Waters: Using the Qualitative Habitat Evaluation Index (QHEI). Ohio EPA, Division of Surface Water, Groveport, OH.
Rapport, D.J., 1989. What constitutes ecosystem health? Perspect. Biol. Med. 33 (1), 120–132.
Schofield, N.J., Davies, P.E., 1996. Measuring the health of our rivers. WATER-MELBOURNE THEN ARTARMON 23, 39–43.
Smirnov, N., 1948. Table for estimating the goodness of fit of empirical distributions. Ann. Math. Stat. 19 (2), 279–281.
Spearman, C., 1904. The proof and measurement of association between two things. Am. J. Psychol. 15 (1), 72–101.
Stephens, W.W., Farris, J.L., 2004. Instream community assessment of aquaculture effluents. Aquaculture 231 (1-4), 149–162.
Stockdale, C.A., Bozzini, C., Macdonald, S.E., Higgs, E., 2015. Extracting ecological information from oblique angle terrestrial landscape photographs: performance evaluation of the WSL Monoplotting tool. Appl. Geogr. 63, 315–325.
Stubauer, I., Hering, D., Korte, T., Hoffmann, A., Brabec, K., Sharma, S., ... Sharma, M.P., 2010. The development of an assessment system to evaluate the ecological status of rivers in the Hindu Kush-Himalayan region: introduction to the special feature. Hydrobiologia 651 (1), 1–15.
Tang, T., Cai, Q., Liu, J., 2002. River ecosystem health and its assessment. J. Appl. Ecol. 13 (9), 1191–1194.
Van der Hoort, B., Ehrsson, H.H., 2016. Illusions of having small or large invisible bodies influence visual perception of object size. Sci. Rep. 6.
Wang, S., Fu, B., Piao, S., Lü, Y., Ciais, P., Feng, X., Wang, Y., 2016. Reduced sediment transport in the Yellow River due to anthropogenic changes. Nat. Geosci. 9 (1), 38–41.
Wang, X., Ren, L., Jiao, F., Liu, W., 2017. The ecological risk assessment and suggestions on heavy metals in river sediments of Jinan. Water Sci. Technol. 76 (8), 2177–2187.
Wei, M., Zhang, N., Zhang, Y., Zheng, B., 2009. Integrated assessment of river health based on water quality, aquatic life and physical habitat. J. Environ. Sci. 21 (8), 1017–1027.
Xu, Z.X., Li, Y.L., 2016. Establishment and application of assessment index system for river health: a case study in the Huntai River basin. South to North Water Transfers and Water Science and Technology 14 (1), 1–9.
Zhang, W., Zhang, X., Li, L., Zhang, Z., 2007a. Urban forest in Jinan City: distribution, classification, and ecological significance. Catena 69 (1), 44–50. https://doi.org/10.1016/j.catena.2006.04.021.
Zhang, Y.X., Li, X.B., Zhang, Y.F., 2007b. Determining vegetation cover based on field data and multi-scale remotely sensed data. J. Plant Ecol. 31 (5), 842–849. https://doi.org/10.17521/cjpe.2007.0106.
Zhang, Q., Jiang, T., Chen, Y.D., Chen, X., 2010. Changing properties of hydrological extremes in south China: natural variations or human influences? Hydrol. Process. 24 (11), 1421–1432.
Zhang, X., Wang, C., Li, E., Xu, C., 2014. Assessment model of ecoenvironmental vulnerability based on improved entropy weight method. Sci. World J. 2014.
Zhao, C., Liu, C., Xia, J., Zhang, Y., Yu, Q., Eamus, D., 2012. Recognition of key regions for the restoration of phytoplankton communities in the Huai River basin, China. J. Hydrol. 420, 292–300.
Zhao, S., Zhou, D., Zhu, C., Qu, W., Zhao, J., Sun, Y., ... Liu, S., 2015. Rates and patterns of urban expansion in China's 32 major cities over the past three decades. Landsc. Ecol. 30 (8), 1541–1559.
Zhao, C.S., Yang, S.T., Liu, C.M., Dou, T.W., Yang, Z.L., Yang, Z.Y., ... Mitrovic, S.M., 2015a. Linking hydrologic, physical and chemical habitat environments for the potential assessment of fish community rehabilitation in a developing city. J. Hydrol. 523, 384–397.
Zhao, C.S., Yang, S.T., Xiang, H., Liu, C.M., Zhang, H.T., Yang, Z.L., ... Lim, R.P., 2015b. Hydrologic and water-quality rehabilitation of environments for suitable fish habitat. J. Hydrol. 530, 799–814.
Zhao, C.S., Zhang, C.B., Yang, S.T., et al., 2017. Calculating e-flow using UAV and ground monitoring. J. Hydrol. 552, 351–365.
Zhao, C.S., Yang, S.T., Liu, J.G., et al., 2018. Linking fish tolerance to water quality criteria for the assessment of environmental flows: a practical method for streamflow regulation and pollution control. Water Res. 141, 96–108.
Zheng, X.Q., Lv, L.N., 2016. A WOE method for urban growth boundary delineation and its applications to land use planning. Int. J. Geogr. Inf. Sci. 30 (4), 691–707.
Zhou, L., He, Z.J., Ooi, T.L., 2013. The visual system's intrinsic bias and knowledge of size mediate perceived size and location in the dark. J. Exp. Psychol. Learn. Mem. Cogn. 39 (6), 19–30.
Zhu, W., Cao, G., Ying, L., Xu, W.L., Shi, M., Qin, L., 2014. Research on the health assessment of river ecosystem in the area of Tumen River Basin. Acta Ecol. Sin. 34 (14), 3969–3977.